$$O_3 + h\nu \rightarrow products$$

Primary Photochemical Transitions

Reaction	ΔH/kJ mol^{-1}	$\lambda_{threshold}$/nm
$O_3 + h\nu \; = \; O(^3P) + O_2(^3\Sigma_g)$ (1)	101	1180
$= O(^3P) + O_2(^1\Delta_g)$ (2)	196	611
$= O(^3P) + O_2(^1\Sigma_g{}^+)$ (3)	258	463
$= O(^1D) + O_2(^3\Sigma_g)$ (4)	291	411
$= O(^1D) + O_2(^1\Delta_g)$ (5)	386	310
$= O(^1D) + O_2(^1\Sigma_g{}^+)$ (6)	448	267
$= 3O(^3P)$ (7)	595	201

Absorption Cross-section Data

Wavelength range/nm	Reference	Comment
245 - 350	Bass and Paur, 1985[1]	(a)
185 - 350	Molina and Molina., 1986[2]	(b)
253.7	Mauersberger et al., 1986[3]	(c)
175 - 360	WMO, 1986[4]	(d)
410 - 760	Burkholder and Talukdar, 1994[5]	(e)
195 - 345	Malicet et al., 1995[6]	(f)
350 – 830	Brion et al., 1998[7]	(f)

Quantum Yield Data

Measurement	λ/nm	Reference	Comment
$\phi[O(^3P)]$	275	Fairchild et al., 1978[8]	(g)

$\phi[O(^3P)]$	266	Sparks *et al.*, 1995[9]	(h)
$\phi[O(^1D)]$	297.5- 325	Brock and Watson, 1980[10]	(i)
$\phi[O(^1D)]$	266	Brock and Watson, 1980[11]	(j)
$\phi[O(^1D)]$	248	Wine and Ravishankara., 1983[12]	(k)
$\phi[O(^1D)]$	248, 308	Greenblatt and Wiesenfeld, 1988[13]	(l)
$\phi[O(^1D)]$	275 - 325	Trolier and Wiesenfeld, 1988[14]	(m)
$\phi[O(^1D)]$	222, 193	Turnipseed *et al.*, 1991[15]	(n)
$\phi[O(^1D)]$	221 - 243	Cooper *et al.*, 1993[16]	(o)
$\phi[O_2(^1\Delta_g)]$	300 - 322	Ball and Hancock, 1995[17]	(p)
$\phi[O_2(^1\Delta_g)]$	287 - 331	Ball *et al.*, 1995[18]	(q)
$\phi[O_2(^1\Delta_g)]$	300 - 322	Ball, Hancock and Winterbottom, 1995[19]	(r)
$\phi[O(^1D)]$	300 - 355	Armerding, Comes and Schulke, 1995[20]	(s)
$\phi[O(^1D)]$	248	Amimoto *et al.*, 1980[21]	(t)
$\phi[O(^1D)), O(^3P)]$	308 - 326	Takahashi, Matsumi and Kawasaki, 1996[22]	(u)
$\phi[O(^1D)]$	300 - 328	Ball *et al.*, 1997[23]	(v)
$\phi[O(^1D)]$	308	Talukdar *et al.*, 1997[24]	(w)
$\phi[O(^1D)]$	305 – 329	Takahashi *et al.*, 1998[25]	(x)
$\phi[O(^1D)]$	289 – 329	Talukdar *et al.*, 1998[26]	(y)
$\phi[O(^1D)]$	301 - 375	Bauer, D'Ottone and Hynes, 2000[27]	(z)
$\phi[O(^1D)]$	295 – 338	Smith, Molina and Molina, 2000[28]	(aa)
$\phi[O(^1D)]$	297 – 305	Taniguchi, Takahashi and Matsumi, 2000[29]	(bb)

___

Comments

a) Measured at 226–298 K with spectral resolution of 0.07 nm.

b) Measured at 200–300 K with spectral resolution of 0.025 nm. Relative values normalised to a value of 1147×10^{-20} cm^2 at the 253.65 nm mercury line.

c) Measured at 297 K and later (reference 7) at 195–351 K on the 253.65 nm mercury line.

d) Critical review of all published data. Recommended values given for standard spectral intervals from 175–360 nm for 203 and 273 K.

e) Measured with a diode array. Cross-sections independent of temperature.

f) Absolute cross sections for O$_3$ absorption in the range 195–345 nm measured at high resolution ($\Delta\lambda$ = 0.01–0.02 nm) using a conventional absorption cell–monochromator combination, with ozone measured manometrically. The temperature dependence of the absorption in the Hartley and Huggins bands was also measured over the range 218–295 K. A small increase in σ with decreasing temperature (1.0% over the whole temperature range) was observed at λ = 253.65 nm, near the maximum in the Hartley band; at 298 K, σ(253.65 nm) = $(113.05 \pm 1.1)\times10^{-19}$ cm^2 molecule^{-1}. In the Huggins bands (300–345 nm) there is a larger temperature dependence (up to 50%), which increases progressively to longer wavelengths. In contrast to the Hartley band there is a decrease in σ with decreasing temperature. The second paper from this group presents absorption spectra measurements for the ozone molecule in the 350–830 nm region, including the Chappuis bands.

g) Photofragment spectroscopy of O$_3$; co-product is O$_2(^3\Sigma^-)$; $\phi(1) = 0.1$.

h) High resolution photofragment spectroscopy giving $\phi(1) = 0.1$.

i) Laser photolysis of O_3 - N_2O mixtures; NO product of $O(^1D)$ reaction with N_2O measured by chemiluminescence from NO_2.

j) Laser flash photolysis; $O(^3P)$ by RF; $\phi(1) = 0.12\pm0.02$ at 266 nm.

k) Laser flash photolysis; $O(^3P)$ by RA; $\phi(1) = 0.15\pm0.02$ at 248 nm.

l) Laser photolysis at 248 nm and 308 nm; $O(^3P)$ by RF; $\phi[O(^1D)] = 0.94\pm0.01$ at 248 nm, $\phi[O(^1D)] = 0.79\pm0.02$ at 308 nm.

m) Laser photolysis of O_3–N_2O mixtures; $O(^1D)$ quenching by CO_2 monitored by infrared chemiluminescence from CO_2.

n) Laser photolysis; $O(^3P)$ by RF; $\phi[O(^3P)] = 0.12\pm0.02$; $\phi[O(^1D)] = 0.87$ at 222 nm.

o) Laser photolysis; $O(^1D)$ detected by weak 630 nm fluorescence emission from $O(^1D) \rightarrow O(^3P)$. Relative $\Phi[O(^1D)]$ normalised to $\phi[(O^1D)] = 0.87$ at 222 nm of Turnipseed et al.[15]

p) Relative quantum yields of $O_2(^1\Delta)$ from laser photolysis of O_3 in the range $300 < \lambda < 322$ nm measured by [2 + 1] resonance enhanced multiphoton ionisation (REMPI) at 227K. For $\lambda > 309$ nm, $\phi[O_2(^1\Delta)]$ at 227 K falls more rapidly than observed at 298K (Ball et al.[30]), confirming that internal energy of O_3 contributes to formation of $O_2 (^1\Delta)$, just beyond the 310 nm threshold for spin allowed production of the two singlet products of channel (5). At $\lambda > 320$ nm, $\phi[O_2(^1\Delta)]$ was approximately equal at the two temperatures, and substantially larger than the then current measurements of $\phi(O^1D)$ suggesting a spin forbidden channel for $O_2 (^1\Delta)$ production, e.g. channel (2), with $\phi(2) = 0.1$ at 320 nm.

q) Kinetic energies of the $O_2 (^1\Delta)$ fragment of O_3 photolysis in the range 287.57 and 331.52 nm measured by time-of-flight mass spectrometry. Between 308 and 318 nm dissociation is dominated by the spin allowed dissociation channel (5). At longer wavelengths, photofragments with higher kinetic energies are produced, consistent with the occurrence of the spin forbidden process, channel (2).

r) Data for $\phi[O_2(^1\Delta)]$ temperature dependence reported in earlier publications[17,18,30] were compared with earlier data for $\phi[O(^1D)]$. At 300–309 nm there is no temperature dependence of the yield of either photo-product. In the fall-off region, 307–319 nm, there is good agreement between the measured yields of $O_2(^1\Delta)$ and modelling calculations by Michelson et al.[31] which take into account dissociation of internally excited ozone molecules for the formation of $O(^1D)$.

s) $\phi[O(^1D)]$ in the wavelength range 300–330 nm and at 355 nm determined indirectly by observation of the LIF of OH produced by the reaction of photofragment $O(^1D)$ with H_2O. $\phi[O(^1D)]$ was determined to be unity at 302.5 nm decreasing to 0.6 at 310 nm with a characteristic 'saddle' point at 315 nm and with a long wavelength tail extending to a threshold between 331 and 333 nm. No $O(^1D)$ was detected at 355 nm.

t) Laser flash photolysis; $O(^3P)$ by RA; $\phi(1) = 0.15\pm0.02$ at 248 nm.

u) The photo fragment yields spectra of $O(^1D)$ and $O(^3P)$ produced in the photodissociation of O_3 in the Huggins band system over the range 308–326 nm were determined using vacuum ultraviolet LIF. The $O(^3P)$ yield exhibited vibrational structure as in the absorption spectrum

in the Huggins band, whilst $O(^1D)$ showed a smooth dependence on wavelength. The quantum yield of $O(^1D)$ was calculated assuming $\phi[O(^1D) + O(^3P)] = 1$. Using the absorption spectrum of Molina and Molina[2] $\phi[O(^1D)]$ showed a distinct 'tail' for the region beyond the threshold for channel (5) at 310 nm, as had been reported in some previous studies (Brock and Watson[10]; Trolier and Wiesenfield[14]), and in the co-product from the spin allowed channel (5), $O_2 (^1\Delta)$, reported by Ball and coworkers[17-19,30]. The 'tail' in $\phi[O(^1D)]$ in the wavelength range 310–321 nm is attributed to hot band excitation of the repulsive limb of the excited state ($^1B_2$ or $^2A_1$) correlating with the singlet products. The non-zero formation of $O(^1D)$ at $\lambda > 321$ nm was tentatively attributed to the spin forbidden process producing $O(^1D) + O_2 (^3\Sigma_g^-)$.

v) Relative quantum yields of $O(^1D)$ determined by REMPI detection of $O(^1D)$ following laser photolysis of O_3 between 300 and 328 nm. Results confirm the tail in the quantum yield extending to wavelengths beyond the thermodynamic threshold at 310 nm, which is attributed to the occurrence of both spin allowed and spin forbidden processes. Absolute quantum yields were obtained by normalisation to a constant value of $\phi = 0.95$ in the range 300–305 nm as recommended by NASA[33].

w) Temperature dependence of quantum yields of $O(^1D)$ following laser photolysis of O_3 at 308 nm and 248 nm between 200–320 K. $O(^1D)$ determined indirectly by 1) conversion to $O(^3P)$ followed by RF detection; 2) conversion to OH/OD, followed by LIF detection. At 308 nm, $\phi[O(^1D)]$ decreased very slightly with temperature from 0.79 at 298 K to 0.73 at 200 K, whilst at 248 nm $\phi[O(^1D)]$ was independent of temperature.

x) Wavelength and temperature dependence of quantum yields of $O(^1D)$ following laser photolysis of O_3 between 305–329 nm and at 295 and 227 K. The photofragment yield spectra of $O(^1D)$ and $O(^3P)$ were determined using vacuum ultraviolet LIF and converted to absolute quantum yields by matching to the O_3 absorption spectrum of Malicet et al.,[6] at the two temperatures and assuming $\phi[O(^1D) + O(^3P)] = 1$. Doppler profiles of nascent $O(^1D)$ were measured, providing information on the dissociation processes. The results are consistent with a dominant hot band contribution at $310 < \lambda < 321$ nm, and with occurrence of the spin forbidden process at $\lambda > 318$ nm producing $O(^1D) + O_2(^3\Sigma_g^-)$ with $\phi = 0.08$.

y) Temperature and wavelength dependence of quantum yields of $O(^1D)$ following laser photolysis of O_3 between 289 - 329 nm at 203–320 K. $O(^1D)$ determined indirectly by *1)* conversion to $O(^3P)$ followed by RF detection; *2)* conversion to OH/OD followed by LIF detection. Absolute values of $\phi[O(^1D)]$ were based on a value of $\phi = 0.79$ at 308 nm, and temperature independent values of $\phi = 0.89\pm0.02$ at $289 < \lambda < 305$ nm and $\phi = 0.06$ for the spin forbidden process at $\lambda > 318$ nm.

z) Relative quantum yields for $O(^1D)$ between 305 and 375 nm at 298 and 273 K. $O(^1D)$ measured indirectly via LIF detection of vibrationally excited OH produced in $O(^1D) + H_2$ reaction. Use of blue shifted LIF gave high detection sensitivity and eliminated probe laser interference. Significant temperature dependent $O(^1D)$ quantum yield at $\lambda = 310$–325 nm confirmed. Between 325 and 375 nm a temperature independent quantum yield of $\phi = 0.064\pm0.006$ observed, which is assigned to the spin forbidden channel (4). This study

supersedes and extends earlier work by this group published by Silvente *et al.*[32], which reached similar conclusions.

aa) Quantum yields for $O(^1D)$ from broadband photolysis of ozone in wavelength range 295–338 nm and temperatures 226 – 298 K. $O(^1D)$ detected by CIMS and absolute quantum yields were based on a value of $\phi = 0.79$ at 308 nm. At λ = 312–324 nm the $O(^1D)$ quantum yield was temperature dependent. Between 328 and 338 nm a temperature independent quantum yield of $\phi \sim 0.12$ was observed, which is assigned to the spin forbidden channel (4).

bb) Wavelength dependence of quantum yields of $O(^1D)$ following laser photolysis of O_3 between 297–316 nm and at 295 K. The photofragment yield spectra of $O(^1D)$ and $O(^3P)$ were determined using vacuum ultraviolet LIF. The photofragment yield spectra of $O(^3P)$ were used to determine quantum yields of $O(^1D)$ between 297–305 nm, which were almost independent of photolysis wavelength in this range ($\phi = 0.89$).

Preferred Values

Ozone absorption cross-sections averaged over spectral intervals

int #	λ/nm	$10^{20}\sigma/cm^2$ 273 K	int #	λ /nm	$10^{20}\sigma/cm^2$ 273 K	$10^{20}\sigma/cm^2$ 203 K
1	175.4-177.0	81.1	31	238.1-241.0	797	797
2	178.6	79.9	32	243.9	900	900
3	180.2	78.6	33	246.9	1000	1000
4	181.8	76.3	34	250.1	1080	1085
5	183.5	72.9	35	253.2	1130	1140
6	185.2	68.8	36	256.4	1150	1160
7	186.9	62.2	37	259.7	1120	1130
8	188.7	57.6	38	263.2	1060	1060
9	190.5	52.6	39	266.7	965	959
10	192.3	47.6	40	270.3	834	831
11	194.2	42.8	41	274.0	692	689
12	196.1	38.3	42	277.8	542	535
13	198.0	34.7	43	281.7	402	391
14	200.0	32.3	44	285.7	277	267
15	202.0	31.4	45	289.9	179	173
16	204.1	32.6	46	294.1	109	104
17	206.2	36.4	47	298.5	62.4	58.5
18	208.3	43.4	48	303.0	34.3	31.6
19	210.5	54.2	49	307.7	18.5	16.6
20	212.8	69.9	50	312.5	9.80	8.67
21	215.0	92	51	317.5	5.00	4.33
22	217.4	119	52	322.5	2.49	2.09
23	219.8	155	53	327.5	1.20	0.937
24	222.2	199	54	332.5	0.617	0.471
25	224.7	256	55	337.5	o.274	0.198
26	227.3	323	56	342.5	0.117	0.077
27	229.9	400	57	347.5	0.059	0.017
28	232.6	483	58	352.5	0.027	-
29	235.3	579	59	357.5	0.011	-
30	238.1	686	60	362.5	0.005	-

$\sigma = (1143 \pm 15)$ x 10^{-20} cm^2 molecule^{-1} at 253.7 nm at 298 K

$\sigma = (1154 \pm 15)$ x 10^{-20} cm^2 molecule^{-1} at 253.7 nm at 220 K

Ozone absorption cross-sections in the visible spectral region*

λ/nm	$10^{23}\sigma$/cm^2	λ/nm	$10^{23}\sigma$/cm^2
410	1.2	560	394
420	2.2	580	459
440	11.2	600	511
460	32.8	620	400
480	68.4	640	296
500	122	660	209
520	182	680	136
540	291	700	91

σ is independent of temperature in the region 410–700 nm.

* Values are for specific wavelengths given; they are not averaged over wavelength ranges.

Quantum Yields for O(^{1}D) production from O$_3$ photolysis at 298 K

Wavelength/nm	ϕ[O(^{1}D)]	Wavelength/nm	ϕ[O(^{1}D)]
305	0.900	317	0.222
306	0.884	318	0.206
307	0.862	319	0.187
308	0.793	320	0.166
309	0.671	321	0.146
310	0.523	322	0.128
311	0.394	323	0.113
312	0.310	324	0.101
313	0.265	325	0.092
314	0.246	326	0.086
315	0.239	327	0.082
316	0.233	328	0.080

$220 < \lambda$/nm < 305: ϕ[O(^{1}D)] = 0.90; ϕ[O(^{3}P)] = 0.10

$330 < \lambda$/nm < 370: ϕ[O(^{1}D)] = 0.080; ϕ[O(^{3}P)] = 0.92

Temperature dependence of Quantum Yields for O(^{1}D) production from O$_3$ photolysis

For 306 < λ/nm < 328 and 200 < T/K< 320):

$$\Phi(\lambda,T)=\left\{\frac{q_1}{q_1+q_2}\right\}\times A_1\times\exp\left\{-\left(\frac{X_1-\lambda}{\omega_1}\right)^4\right\}+\left\{\frac{q_2}{q_1+q_2}\right\}\times A_2\times\left\{\frac{T}{300}\right\}^2\exp\left\{-\left(\frac{X_2-\lambda}{\omega_2}\right)^2\right\}$$

$$+A_3\times\left\{\frac{T}{300}\right\}^{1.5}\exp\left\{-\left(\frac{X_3-\lambda}{\omega_3}\right)^2\right\}+c$$

where

$$q_i=\exp\left(-\frac{v_i}{RT}\right)$$

A_1 = 0.8036; A_2 = 8.9061; A_3 = 0.1192; X_1 = 304.225; X_2 = 314.957; X_3 = 310.737;

ω_1 =5.576; ω_2 = 6.601; ω_3 = 2.187; v_1 = 0; v_2 = 825.518; c = 0.0765;

We recommend this expression for use in the wavelength and temperature range given above. It should not be used outside this range. ϕ[O(^{1}D)] is independent of temperature in the range 220 < λ/nm < 305 and 330 < λ/nm < 370.

Comments on Preferred Values

Absorption cross-sections

The recommended absorption cross-section values at 273 K for the wavelength range 175–362 nm are averaged values for the standard spectral intervals used in atmospheric modelling calculations. These values have been adopted from earlier evaluations (NASA 1994[33], IUPAC, 1996[34], which accepted the values tabulated in the WMO 1986 review[4], except for the region 185–225 nm where the values were taken from the study of Molina and Molina.[2]

Recommended values at 203 K in the Huggins bands are also taken from the WMO 1986 review and are based on the data of Bass and Pauer.[1]

The new work of Malicet et al.[6] provides detailed data on the absolute absorption cross sections of ozone and their temperature dependence (218–295 K), over the wavelength range 195–345 nm. The measurements are at sufficient resolution to resolve the vibrational structure in the Huggins bands. The data are generally in excellent agreement with earlier measurements, although there are small differences in detail in specific regions of the spectrum. At wavelenghts below 240 nm the cross-sections are identical with those of Molina and Molina[2], confirming the basis of the recommended values in this range. In the range 240–335 nm the new data are between 1.5% and 3.0% lower than those of Molina and Molina[2] but about 1.5% higher than those of Yoshino et al.,[35] but are very close to the data of Bass and Pauer[1] up to 310 nm. In the Huggins bands ($\lambda > 310$ nm), shifts of +0.05 nm in the vibrational structure are apparent in the Bass and Pauer data, which may be due to error in the wavelength calibration. This gives rise to small but significant differences in the individual cross-sections and their temperature dependence. Nevertheless the small differences do not influence the averaged cross-sections sufficiently to warrant revision of the recommended values for calculation of the atmospheric photoabsorption rates of ozone in the Huggins bands. For cross-sections at high resolution, the data of Malicet et al. [6], which are available in digital form from the authors, is recommended.

Malicet et al [6] observed a weak temperature dependence near the maximum in the Hartley band, leading to an increase of approximately 1% in σ between 295 and 218 K, in agreement with earlier work of Molina and Molina[2] and Barnes and Mauersberger.[36] The values recommended for the cross section at 253.7 nm have been obtained by averaging the data of Daumont et al.[36], Malicet et al.[6], Hearn[37], Molina and Molina[2] and Mauersberger et al.[3,36] The new recommendation is slightly lower than previously given on the basis of the last three studies.

Ozone cross sections in the Chappius bands (450-750 nm), which are independent of temperature, are taken from Burkholder and Talukdar.[5] The values reported by Brion et al. [6] are in good agreement.

Quantum Yields

A wealth of data from studies cited in the table for the quantum yield for $O(^1D)$ production and its co-product, $O_2(^1\Delta_g)$, in the spin allowed dissociation channel (5), give clear evidence for substantially enhanced dissociation into electronically excited products beyond the threshold at 310 nm. This is attributed to the contribution of vibrational energy contained in ground state O_3

molecules. Recent measurements also show that significant $O(^1D)$ production occurs at $\lambda = 320$–370 nm which is attributed to the spin forbidden channel (4). The new data up to 1997 were considered in IUPAC (Supplement VI), where a complete revision in the recommended quantum yields for $O(^1D)$ production at 298 K was made, which included the 'tail' in $\phi[O(^1D)]$ at wavelengths beyond 312 nm (see Figure 1). The recommended values for $\phi[O(^1D)]$ covering the range 300–335 nm at 298 K, were obtained by taking a smooth curve through the mean of the experimental values reported by Brock and Watson[10], Trolier and Wiesenfeld[14], Armerding *et al.*[20], Takahashi *et al.*[22] and Silvente *et al.*[32](for $\lambda > 325$ nm only). In the absence of direct measurements of $\phi[O(^1D)]$ at other temperatures, no recommendation was made for the temperature dependence. The 'tail', was partly attributed to the involvement of vibrationally excited ozone, implying a fall off in $\phi[O(^1D)]$ with temperature in the important region between 308–320 nm. This has now been confirmed in several studies.

Since 1997 there have been six new studies[23-28] in which $\phi[O(^1D)]$ was determined, the data now covering a range of temperature from 200 to 320 K and wavelength from 289 to 375 nm. The results of these studies at 298 K are plotted, together with the earlier data cited above, in Figure 1. The studies are all in good agreement and support $O(^1D)$ production beyond the threshold at 310 nm. Recently, a rigorous evaluation of the data has been conducted by a group involving the principal investigators of these recent studies (Matsumi *et al.*[38]). The group had access to all experimental data and were able to harmonise and renormalise the quantum yield values to eliminate systematic errors. The O_3 absorption spectrum of Malicet *et al.*[6] was used in the renormalisation.

The recommendations for the $\phi[O(^1D)]$ were derived using the following procedures. First $\phi[O(^1D)]$ at 308 nm and 298 K was set at 0.79. This was based on the measurements of Greenblatt and Wiesenfeld,[13] Talukdar *et al.*[24], and Takahashi *et al.*[22,25]. A wavelength dependence of $\phi[O(^1D)]$ at 298 K between 306 and 328 nm was derived by averaging the renormalised data from Brock and Watson[10], Trolier and Wiesenfeld[14], Armading *et al.*,[20] Takahashi *et al.*,[22] Ball *et al.*,[23] Talukdar *et al.*,[24,26] Bauer *et al.*,[27] and Smith *et al.*[28]

The recent studies of Talukdar *et al.*,[26] Taniguchi *et al.*[29] and Smith *et al.*[28] show $\phi[O(^1D)]$ values in the range 290–305 nm of around 0.90. The renormalised values of Trolier and Wiesenfeld[14], Armerding *et al.*,[20] Takahashi *et al.*,[22] Ball *et al.*[23] also showed values in this region. Matsumi *et al.*[39] therefore recommended a value of $\phi[O(^1D)] = 0.90\pm0.09$ for $290 < \lambda < 305$ nm. We adopt these recommendations as our preferred values at 298 K, which are listed in the Table.

There are several studies (Brock and Watson,[11] Amimoto *et al.*,[21] Wine and Ravishankara,[13] Greenblatt and Wiesenfeld,[13] Turnipseed *et al.*,[15] Cooper *et al.*,[16] Talukdar *et al.*[26]) which

show that, in the wavelength range 222–275 nm, $\phi[O(^1D)]$ is between 0.85 and 0.90 without significant variation. Fairchild et al.[8] and Sparks et al.[9] report significant $O(^3P)$ production in the Hartley Band at 275 and 266 nm. We therefore recommend a value of $\phi[O(^1D)]$ = 0.90±0.05 and $\phi[O(^3P)]$ = 0.10±0.05 for the entire range 220< λ <305 nm.

Recent data on the temperature dependence of $\phi[O(^1D)]$ (Takahashi et al.,[25] Talukdar et al.,[26], Bauer et al.,[27] Smith et al.[28]) confirms that the yield is temperature dependent at wavelengths > 308 nm, as indicated by earlier indirect measurements of Lin and DeMore[40] (275–320 nm) at 233 K and Kuis et al.[41] (313 nm) in the range 221–293 K, and measurements of Ball et al [17,18,19] of $\phi[O_2(^1\Delta_g)]$ at 298 K and 227 K. However the recent observations show that at all temperatures, $\phi[O(^1D)]$ and $\phi[O_2(^1\Delta_g)]$ decline to a limiting value of ~ 0.1. Evidence from the time-of-flight experiments of Ball et al.[18] and the Doppler profiles of nascent $O(^1D)]$ (Takahashi et al.,[42,25] Denzer et al.[43]) strongly points to a contribution from the spin forbidden channel (2). O'Keeffe et al.[44] have observed nascent $O_2(b^1\Sigma_g)$ photofragments from O_3 photodissociation between 335 and 352 nm, indicating a contribution from channel (3) in this region. These channels involve ground state O_3 and are, therefore, unlikely to be temperature dependent.

Experiments show that at wavelengths below 305 nm, $\phi[O(^1D)]$ is invariant with temperature. At 308 nm, Matsumi et al.[39] recommend the following expression based on the recent data[25,26,27,28]:

$$\phi \text{ (308 nm, T)} = 6.10 \text{ x } 10^{-4}T + 0.608$$

Matsumi et al.[39] have fitted the renormalised quantum yield data of Brock and Watson,[10] Trolier and Wiesenfeld,[14] Armerding et al.,[20] Takahashi et al.,[22,25] Ball et al.,[23] Talukdar et al.,[24,26] Bauer et al.,[27] and Smith et al.[28] for 306 < λ/nm < 328 and 200 < T/K< 320 with an expression using three Gaussian terms and a constant term representing the spin- forbidden channel(4). Figure 2 shows the quantum yields calculated with this expression at 203, 298 and 320 K, together with selected experimental data. This expression, which is given in the preferred values above, is recommended for use in the wavelength and temperature range given above. It should not be used outside this range.

In the Chappius bands, dissociation to ground state products via reaction (1) is generally assumed to occur with a quantum yield of 1. Recent theoretical calculations[43] lend support for this.

Two field studies in which chemical actinometer measurements of $J(O^1D)$ have been compared with values calculated from simultaneously measured actinic flux spectra have been reported

recently by Mueller *et al.*, 1995[45], and by Shetter *et al.*,1996[46]. Both support the existence of the long wavelength tail in $\phi(O^1D)$ in atmospheric photolysis rates.

References

1. A M Bass and R J Paur, Atmospheric Ozone, Proceedings of Quadrennial Ozone Symposium in Halkidiki, Greece, (D Reidel Publishing Co.,1985) pp 606 - 616.

2 M.J. Molina and L.T. Molina, J. Geophys. Res. **91**, 14501 (1986).

3 K. Mauersberger, J. Barnes, D. Hanson and J. Morton, Geophys. Res. Lett., **13**, 671 (1986).

4 WMO Global Ozone Research and Monitoring Project Report No.16: Atmospheric Ozone 1985, Chapter 7 (1986).

5 J.B. Burkholder and R.K. Talukdar, Geophys. Res. Lett. **21**, 581 (1994).

6 J. Malicet, D. Daumont, J. Charbonnier, C. Parisse, A. Chakir and J. Brion, J. Atm. Chem. **21**, 263 (1995).

7 J. Brion, A. Chakir, J. Charbonnier, D. Daumont, C. Parisse, J. Malicet, J. Atmos. Chem. **30**, 291 (1998).

8 C.E. Fairchild, E.J. Stone and G.M. Lawrence, J. Chem. Phys. **69**, 3262 (1978).

9 R.K. Sparks, L.R. Carlson, K. Shotobake, M.L. Kowalczyk and Y.T. Lee, J. Chem. Phys. **72**, 1401 (1980).

10. J.C. Brock and R.T. Watson, Chem. Phys. **46**, 477 (1980).

11 J.C. Brock and R.T. Watson, Chem. Phys. Lett. **71**, 371 (1980).

12   P.H. Wine and A.R. Ravishankara., Chem. Phys. Lett. **96**, 129 (1983).

13 G.D. Greenblatt and J.R.Wiesenfeld, J. Chem. Phys., **78**, 4924 (1983).

14 M. Trolier and J.R. Wiesenfeld, J. Geophys. Res. **D93**, 7119 (1988).

15 A.A. Turnipseed, G.L. Vaghjianni, T. Gierczak, J.E. Thompson and A.R. Ravishankara, J Chem. Phys. **95**, 3244 (1991).

16 I.A. Cooper, P.J. Niell and J.R. Wiesenfeld, J. Geophys. Res. **98**, 12795 (1993).

17. S.M. Ball and G. Hancock, Geophys. Res. Lett. **22**, 1213 (1995).

18. S.M. Ball, G. Hancock, J.C. Pinot de Moira, C.M. Sadowski and F. Winterbottom, Chem. Phys. Lett. **245**, 1 (1995).

19. S.M. Ball, G. Hancock and F. Winterbottom, J.Chem.Soc. Faraday Discussions **100**, 215 (1995).

20. W. Armerding, F.J. Comes and B. Schülke, J. Phys. Chem. **99**, 3137 (1995).

21. S.T. Amimoto, A.P. Force, J.R. Wiesenfeld and R.H. Young, J. Chem. Phys. **73**, 3640 (1980).

22. K. Takahashi, Y. Matsumi and K. Kawasaki, J. Phys. Chem. **100**, 4084 (1996).

23. S.M. Ball, G. Hancock, S. E. Martin and J. C. Pinot de Moira, Chem. Phys. Lett. **264**, 531 (1997).

24 R.K. Talukdar, M.K. Gilles, F.Battin-Leclerc, A.R. Ravishankara, J.-M. Fracheboud, J.J. Orlando and G.S. Tyndall, Geophys. Res. Lett. **24**, 1091, (1997).

25. K. Takahashi, N. Taniguchi, Y. Matsumi, M. Kawasaki, and M.N.R Ashfold, J. Chem. Phys. **108**, 7161 (1998).

26 R.K. Talukdar, C.A. Longfellow, M.K. Gilles and A.R. Ravishankara, Geophys. Res. Lett. **25**, 143 (1998).

27 D. Bauer, L.D'Ottone and A.J. Hynes, Phys. Chem. Chem. Phys. **2**, 1421 (2000).

28 G.D.Smith, L.T. Molina and M.J. Molina, J. Phys. Chem. A, **104**, 8916 (2000).

29 N. Taniguchi, K. Takahashi, and Y. Matsumi, J. Phys. Chem. A, **104**, 8936 (2000).

30 S.M. Ball, G. Hancock, I.J. Murphy and S.P. Rayner, Geophys. Res. Lett., **20**, 2063 (1993).

31 H.A. Michelson, R.J. Salawitch, P.O. Wennberg and J.G. Anderson, Geophys. Res. Lett., **21**, 2227 (1994).

32 E. Silvente, R.C. Richter, M. Zheng, E.S. Saltzman and A.J. Hynes, Chem. Phys. Lett., **264**, 309-315 (1997).

33 NASA Evaluation No 12, 1997 (see references in Introduction).

34 IUPAC Supplement VI, 1997 (see references in Introduction).

35 K. Yoshino, J.R. Esmond, D.E. Freeman and W.H. Parkinson, J. Geophys. Res. **98**,5205 (1993).

36. J. Barnes and K Mauersberger, J Geophys. Res. **92**, 14861 (1987).

37 D.D. Daumont, J. Brion, J. Charbonnier and J. Malicet, J. Atmos. Chem. **15**, 145 (1992).

38 A.G. Hearn, Proc. Phys. Soc. London **78**, 932 (1961).

39 Y. Matsumi, F.J. Comes, G. Hancock, A. Hofzumahaus, A.J Hynes, M. Kawasaki, A.R. Ravishankara, J. Geophys. Res. *in press* 2001.

40 C-L. Lin and W.B. DeMore, J. Photochem. **2**, 161 (1973).

41 S. Kuis, R. Simonaitis and J. Heicklen, J. Geophys. Res. **80**, 1328 (1975).

42 K. Takahashi, M. Kishigami, Y. Matsumi, K. Kawasaki and A. Orr-Ewing, J. Chem. Phys. **105,** 5290 (1996).

43 W. Denzer, G. Hancock, J.C. Pinot de Moira, and P.L Tyley, Chem. Phys. Lett. **280**, 496 (1997).

44 P. O'Keeffe, T. Ridley, Sh. Wang, K.P. Lawley, and R.J. Donovan, Chem. Phys. Lett. **298**, 368 (1998).

45 M. Muller, A. Kraus and A. Hofzumahaus, Geophys. Res. Lett. **22**, 679 (1995).

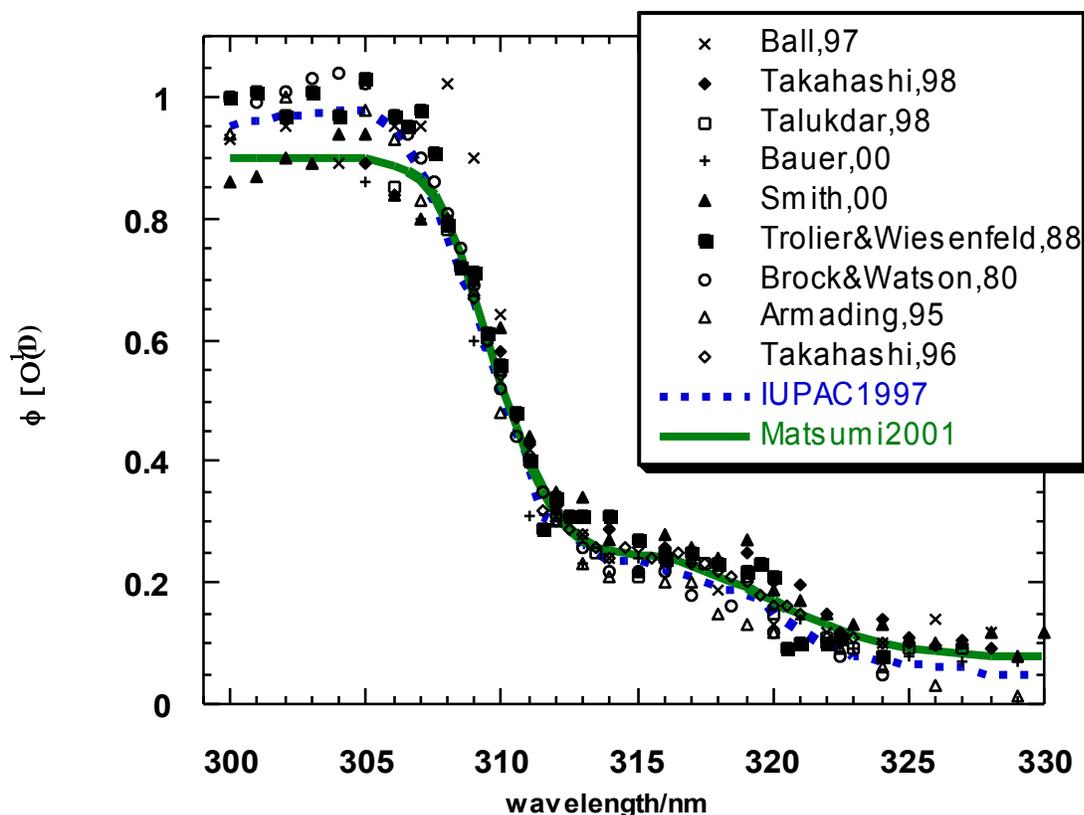46 R.E. Shetter, C.A. Cantrell, K.O. Lantz *et al*., J. Geophys. Res. **101**, 14631 (1996).

Figure 1

Quantum Yields for O(^{1}D) production from O_3 photolysis at 298 K. The data are taken from the cited references without normalisation. The IUPAC recommendation is a mean of the values reported by Brock and Watson,[10] Trolier and Wiesenfeld,[14] Armerding et al.,[20] Takahashi et al.,[22] and Silvente et al.[32] (for $\lambda > 325$ nm only). The recommendation of Matsumi et al.,[39] which is adopted for this IUPAC evaluation, is derived by averaging the renormalised data from Brock and Watson,[10] Trolier and Wiesenfeld,[14] Armading et al.,[20] Takahashi et al.,[22] Ball et al.,[23] Talukdar et al.,[24,26] Bauer et al.,[27] Smith et al.,[28] and Taniguchi et al.[29]

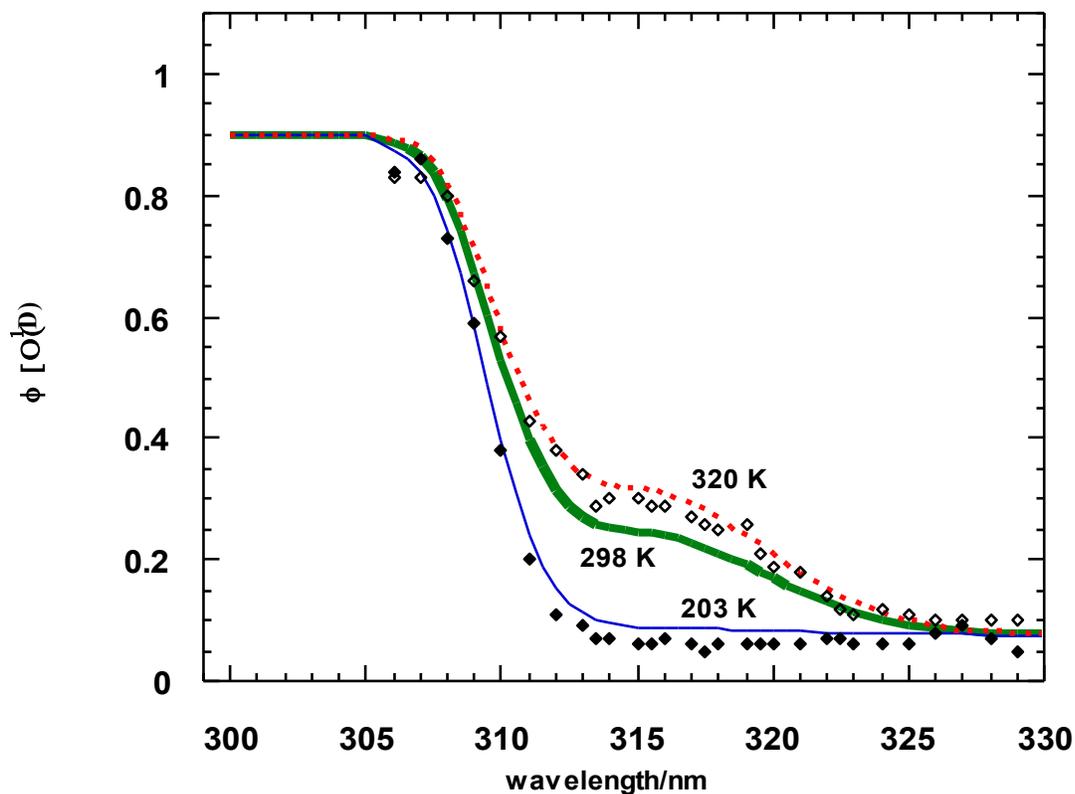**Temperature dependence of ϕ [O(^{1}D)]**

Figure 2

Temperature dependence of Quantum Yields for O(^{1}D) production from O$_3$ photolysis. The curves show values at 202, 298 and 320 K calculated using the expression derived by Matsumi *et al.*[39] using three Gaussian terms and a constant term representing the spin-forbidden channel(4). This expression is given in the preferred values. Selected experimental data from Talukdar *et al.*[26] at 203 and 320 K are also shown.